Assessing Vegetation Change from 2005 to 2024 Using Remote Sensing and Geographic Information Systems: A Case Study of the Phung River Basin, Sakon Nakhon Province

Narathip Ruksajai[1], Phayom Saraphirom[2*] and Worapong Lohpaisankrit[3]

[1, 2]Department of Agricultural Engineering, Faculty of Engineering, Khon Kaen University

[3]Department of Civil Engineering, Faculty of Engineering, Khon Kaen University

payosa@kku.ac.th

Received 20 January 2025

Revised 21 April 2025

Accepted 28 April 2025

Abstract

This study enhances the detection of vegetation changes in Thailand's Phung River Basin, Sakon Nakhon province, by applying the Normalized Difference Vegetation Index (NDVI) within a GIS and remote sensing framework from 2005 to 2024. NDVI, a globally recognized indicator of vegetation health and ecological conditions, was calculated using multi-temporal Landsat imagery. The analysis classified vegetation into five density categories across five time points—2005, 2010, 2015, 2020, and 2024—revealing significant ecological shifts. Dense vegetation increased notably from 11.39% to 20.58%, while areas with moderate and sparse vegetation declined. These changes aligned with demographic trends, including population growth from 2005 to 2020 and a sharp 24% decrease from 2020 to 2024, as well as the implementation of stricter land-use policies. By integrating NDVI-derived analysis, GIS-based spatial modeling, and ΔNDVI change detection, the study substantially improved the monitoring of vegetation dynamics. This approach enabled precise identification of degradation and regeneration zones, offering a practical model for sustainable land management. The methodology presents a scalable tool for other tropical watersheds, supporting regional sustainability strategies across Southeast Asia. The results indicate that vegetation dynamics within the Phung River Basin are closely associated with human-driven activities, notably agricultural expansion and the implementation of land-use regulations. These findings provide essential baseline information to support the development of effective and sustainable forest management policies moving forward.

Keywords: NDVI, Remote Sensing, Landsat Imagery, GIS, Vegetation Change Detection

1. Introduction

Global forest cover is a critical indicator of our planet's environmental health. Natural, non-degradable forests provide numerous functions, such as nutrient recycling, climate regulation, soil stabilization, and waste decomposition, while supporting various recreational opportunities and natural ecosystems [1]. Although forests worldwide still encompass almost 40 million km² [2], they have been gradually declining each year. Similarly, Thailand's natural forests, covering 162,909.04 square kilometers [3], have experienced significant degradation in recent years [4], with biodiversity declining due to excessive resource use [3]. In the context of Thailand, understanding forest change at the watershed level—such as the Phung River Basin—is essential for formulating localized environmental policies.

Due to agricultural and urban growth, particularly in the northeastern region, forest regions in Thailand have seen significant decline in the last few decades. Challenges remain in managing forest encroachment and accurately monitoring changes at the micro-watershed level, despite reforestation efforts and government preservation policies. One such vulnerable area requiring ecological evaluation at the local level is the Phung River Basin. This study focuses on the Phung River Basin to illustrate how rapidly forest cover can deteriorate under the combined pressures of climate change and human activity. The basin, recognized for its rich forest heritage and hydrographic network, currently faces challenges such as illegal logging, overgrazing, land clearing, agricultural expansion, and destructive fires—indicating the urgent need for sustainable forest management strategies [36].

Understanding the evolution of forest cover is paramount for regions experiencing severe degradation, as even minimal changes can directly impact natural resource availability [5]. High spatial resolution satellite data provides a critical advantage in remotely assessing forest cover. As shown in [6], C. Suwanprasit and N. Shahnawaz conducted a comparative analysis of fire-affected forest regions in Thailand's Mae Hong Son and Chiang Mai provinces, with a particular focus on Mae Chaem, Chom Thong, Hod, Mae La Noi, and Mae Sariang districts. Their investigation employed vegetation indicators to evaluate the extent and impact of fire damage across diverse ecological zones. Building on these findings, the present study leverages NDVI, derived from Landsat satellite imagery, as a principal metric for forest cover assessment [7, 8]. Numerous peer-reviewed studies have demonstrated the reliability of NDVI in capturing forest dynamics and ecological viability, particularly in detecting long-term habitat degradation through Landsat-based time-series analysis [7], [8], [29]. It has also been effectively applied to monitor vegetation dynamics in Mediterranean environments using multi-resolution satellite data [16]. Moreover, its utility in detecting forest cover change driven by anthropogenic and environmental factors has been confirmed in localized studies, such as those conducted in the Metekel Zone of Northwest Ethiopia [17]. For example, post-fire forest recovery in Mediterranean regions was examined by Lopes et al. (2024) using NDVI, and the impacts of land use and climate change on the dynamics of forest NDVI in Romania were stressed by Prăvălie et al. (2022). The dependability of NDVI as a remote sensing instrument for assessing environmental changes across diverse settings is emphasized in these studies. NDVI is calculated by examining the red (R) and near-

infrared (NIR) bands' reflectance differences, which drone- or satellite-based sensors can detect [9], [29]. In principle, positive NDVI values indicate vegetation and negative values imply non-vegetated areas, indicating the proportion of plant cover [10].

Utilizing NDVI-derived Landsat data and Geographic Information Systems (GIS), the research intends to examine vegetation changes in the Phung River Basin between 2005 and 2024 and evaluate the effects of human development on forest regions. The quantification of forest degradation is possible using this method and underpins the expansion of approaches to alleviate soil erosion as well as stimulate sustainable administration of the watershed.

1.1 Long-Term Vegetation Analysis: The study utilizes remote sensing and GIS techniques to evaluate changes in vegetation from 2005 to 2024, offering a robust temporal perspective.

1.2 Integration of Diverse Data Sources: The research combined Landsat satellite imagery with field surveys and GIS-based spatial analysis, providing a detailed understanding of vegetation dynamics in the Phung River Basin.

1.3 Practical Environmental Implications: The findings inform resource management strategies aimed at mitigating soil erosion, conserving biodiversity, and guiding sustainable land use planning.

1.4 Extended Temporal Range: Unlike previous work that often focuses on short timeframes, this research covers nearly two decades of vegetative change (2005–2024), enabling a more nuanced understanding of long-term environmental trends.

1.5 Localized Focus with Broader Implications: While it provides a case study of the Phung River Basin, the methodology and outcomes can be adapted and applied to similar watershed regions elsewhere.

1.6 Comprehensive Methodological Approach: The amalgamation of remote sensing, GIS, and field-validation data permits a higher level of accuracy and specificity in monitoring vegetation changes, surpassing standard desktop analyses.

Unlike previous studies that examined short-term NDVI fluctuations, this research offers a 19-year perspective with high classification accuracy, enabling the detection of nuanced ecological transitions in a tropical watershed.

2. Materials and methods

2.1 Area of Study

The Phung River basin, situated in northeastern Sakon Nakhon province, Thailand, is a branch of the Mekong River Basin situated between 16° 20′ 0″-17° 18′ 0″ north latitude and 103° 80′ 0″-104° 16′ 0″ east longitude (Fig. 1). The Nam Un River tributary basin is north, and the Kam River basin is east. The Phung River, from the western mountain range at Phu Sila and Phu Nong Ma, is the basin's main river. The river travels through Phu Phan, Tao Ngoi, and Khok Si Suphan districts before emptying into Nong Han at Ban Don Yang, Lao Po Daeng Sub-district, Sakon Nakhon province. The Phung River, supplies the province with freshwater, runs 76.44 kilometers from Nam Phung Dam to Nong Han. Basin waterways intersect on both sides. In Sakon Nakhon province, the Phung River basin

covers 1,639.60 square kilometers in the Phu Phan District, Tao Ngoi District, Mueang Sakon Nakhon District, and Khok Si Suphan Districts. In the central section, plains with hills transition from high mountains and steep slopes in the upper basin. The basin's lowest part is flat and gradually undulating. The basin's altitude is 300–500 meters above sea level. Typical wind speeds are 2.1 to 3.9 knots or Light Air to Light Breeze. The primary seasonal winds are the northeast and southwest monsoons, from November to February and April to May. Pacific Ocean and South China Sea cyclones and depression storms barely affect Sakon Nakhon. The mountain ranges in Vietnam and Laos slow these gales, weakening them before reaching Thailand. Storms usually bring heavy rain and moderate winds. About two depression storms occur annually [11]. Annual lows and highs are 22.3°C to 31.9°C. The average yearly rainfall in Sakon Nakhon is 1,661.7 mm [11]. Sakon Nakhon province, specifically the Phung River Basin, was selected as the study area due to its ecological sensitivity and diverse topographic characteristics, including mountainous terrains, forested uplands, and fertile lowlands. This area is critical as a headwater basin supplying freshwater for agriculture and local communities. Over recent decades, it has become increasingly susceptible to anthropogenic pressures such as deforestation, agricultural expansion, and land degradation, collectively contributing to significant changes in vegetation cover and ecosystem health.

Moreover, the Phung Basin offers a high temporal continuity of satellite imagery data, particularly from the Landsat program, from 2005 to 2024. This makes it highly suitable for long-term spatiotemporal vegetation analysis using NDVI. The period aligns with notable socio-environmental transitions in the region, including population growth and changing land-use patterns under rural development policies [19].

In terms of tracking forest changes in transitory environments, the Phung River Basin is a beneficial case study from an academic standpoint. Adding to the design of evidence-based reforestation approaches and sustainable environmental planning, the outcomes from this region are generally appropriate to comparable agroecological zones throughout Southeast Asia.

The basin's topography is varied, with flat floodplains downstream, undulating lowlands in the middle, and high mountainous regions in the upper reaches. With a heterogeneous landscape at an altitude ranging between 300 and 500 meters above sea level, vegetation dispersal and the sensitivity of the basin to anthropogenic and climatic pressures are boosted.

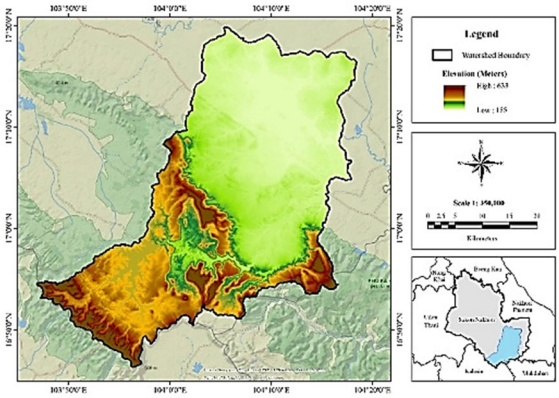

Fig. 1 Phung River Basin study area

2.2 The methodology

The methodology in this study adopts a systematic approach to detect long-term vegetation changes using NDVI over the Phung River Basin from 2005 to 2024. As depicted in Fig. 2, satellite imagery was initially acquired, utilizing Landsat 5 TM for 2005 and 2010 and Landsat 8 OLI-TIRS for 2015, 2020, and 2024, from the USGS Earth Explorer platform. Because of their 30-meter spatial resolution and 16-day revisit cycle, ideal for long-term observation of vegetation in tropical settings distinguished by frequent cloud cover, Landsat 5 and Landsat 8 were chosen, which include sensors offering reliable temporal data over two decades, allowing for the dynamic evaluation of NDVI trends [37]. All imagery underwent preprocessing and processing, including geometric and radiometric corrections, to ensure cross-year comparability and spectral integrity [20], [24]. NDVI was then calculated using the standard formula, as illustrated in Equation 1. The NIR bands, (Band 4 for Landsat 5 and Band 5 for Landsat 8) and the Red band (Band 3 for Landsat 5 and Band 4 for Landsat 8), were extracted from each image to compute NDVI values, which were used to generate NDVI maps for each year (2005, 2010, 2015, 2020, and 2024). Vegetation classification was conducted using the Maximum Likelihood Supervised Classification method, which involved selecting training and validation data from field surveys, thematic maps, and high-resolution imagery from Google Earth [21].

Following classification, an accuracy assessment was conducted through confusion matrices, yielding metrics such as Overall Accuracy and Kappa coefficient to quantify model performance. Using annual NDVI maps, statistical analysis produced maps showing areas of increase or decrease in vegetation cover. Finally, NDVI trend detection across the 19 years provided a temporal perspective on forest change dynamics under anthropogenic and environmental influences [22].

2.2.1 Cloud Masking and Atmospheric Filtering

All satellite images were exposed to a thorough process of cloud masking before NDVI computation in order to confirm the consistency of spectral analysis and reduce interference from the atmosphere, especially in areas with continuous cloud cover. The Function of Mask (Fmask) algorithm [33] was used in this study, which utilizes a programmed, object-based approach purposely constructed to detect and remove atmospheric inconsistencies from Landsat imagery, such as clouds,

cloud shadows, and snow.

To discriminate valid surface reflectance from corrupted pixels, Fmask incorporates spectral thresholding, thermal band assessment, and contextual evaluation, involving spatial adjacency and object morphology. This procedure was created to compensate for the limits of conventional threshold-based cloud detection methods threshold-based cloud detection methods [32], considerably boosting detection accuracy while reducing errors due to omission and commission [31].

This approach has been combined with the United States Geological Survey's (USGS) [34] Landsat Surface Reflectance packages and has been implemented extensively on global remote sensing platforms, such as Google Earth Engine (GEE) [35] and the Earth Resources Observation and Science Processing Archive (ESPA). To manage five Landsat scenes traversing from the years 2005 to 2024, with only clear-sky pixels preserved for NDVI generation, this study applied Fmask version 4.0 using the ERDAS Imagine preprocessing module.

Because cloud-corrupted pixels can misrepresent values for red and near-infrared reflectance, causing inaccurate vegetation signals or understatement of vegetation density, NDVI-based vegetation analysis requires precise cloud masking. Spectral integrity and temporal stability can be ensured by the use of Fmask before NDVI classification, thus allowing for the active assessment of vegetation dynamics across the 19-year period. For long-term ecological evaluations, particularly within multifaceted tropical environments, such preprocessing is essential to preserving the quality of data. To obtain and evaluate NDVI values over time, combined satellite-based remote sensing and Geographic Information Systems (GIS) were used in this study. To obtain NDVI maps, allowing for spatial and temporal appraisal of changes in vegetation across the Phung River Basin, Landsat imagery was managed employing ERDAS Imagine and ArcGIS software. A high level of spatial precision and analytical reliability was confirmed across all observation years using this integrative method, underpinning the consistency of NDVI-based vegetation evaluations in dynamic tropical landscapes.

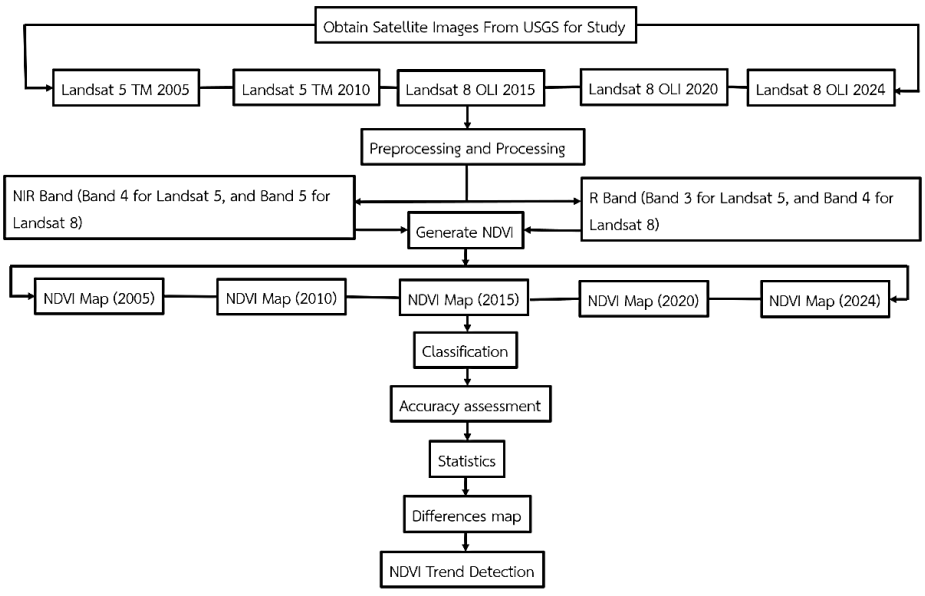

Fig. 2 Flowchart showing the integrated NDVI processing workflow, including satellite image acquisition, preprocessing (e.g., geometric and radiometric corrections), cloud masking via Fmask, NDVI computation, vegetation classification, trend analysis, and validation.

2.3 The collection of data

This research utilized five 30-meter resolution images from the Landsat program from 2005 to 2024, obtained from the US Geological Survey National Center (USGC). The procurement of Landsat 8 OLI coincided with the data collection from Landsat 5 TM and Landsat 8 OLI (Table 1). This study's main satellite images were taken during the dry season, as this season provides the most significant forest cover disparity compared to other kinds of land development. ERDAS Imagine 2020 and ArcGIS Desktop Version 10.7 software were used for image processing. A 30-meter spatial resolution was used, and for all projection system data, UTM Zone 48 North was used.

Table. 1 Satellite Data of Landsat Images Utilized

Satellite	Sensor	Path/Row	Resolution	Date of Acquisition
LANDSAT-5	TM	127/48	30 Meter	2005
LANDSAT-5	TM	127/48	30 Meter	2010
LANDSAT-8	OLI-TIRS	127/48	30 Meter	2015
LANDSAT-8	OLI-TIRS	127/48	30 Meter	2020
LANDSAT-8	OLI-TIRS	127/48	30 Meter	2024

2.4 NDVI Preprocessing and Spectral Analysis

The NDVI ranges were from -1 to 1. The low values suggested unproductive rock, sand, snow areas, and clouds. Moderate values point to shrubs and meadows, while high values indicate extensive vegetation. As stated by [12], the NDVI value for exposed soil is around zero, and negative values relate to wetland areas. NDVI is a vegetation index that evaluates vegetation quantity, quality, and evolution by determining specific bands of the electromagnetic spectrum [13] via the strength of the radiation. The formula used for calculating NDVI was [14]:

$$NDVI = \frac{(NIR - R)}{(NIR + R)} \quad (1)$$

Where:

NIR - Near infrared (Band 4 for Landsat 5, and Band 5 for Landsat 8);

R - Red (Band 3 for Landsat 5, and Band 4 for Landsat 8)

The Vegetation Index was grouped into ranges using the determined Normalized Difference. NDVI values for bare rock, sand, or snow are often relatively low and correlate to classes (no vegetation).

Low levels depict shrubs and grasslands, while intermediate values represent senescent crops, which are moderately vegetated. High to very high NDVI values indicate profuse vegetation [15].

Classifying NDVI values into discrete vegetation density classes allows researchers to detect and monitor landscape-scale vegetation changes with high accuracy and consistency. This method has been widely validated through field calibration, high-resolution remote sensing, and ecological indicators [22].

The five vegetation density classes used in this study were informed by NDVI thresholding approaches described in earlier remote sensing research, which demonstrated their applicability in assessing vegetation structure across diverse ecological settings [23], [28]. These thresholds are typically linked to land cover types and demonstrate efficacy across tropical, temperate, and semi-arid environments, as indicated in Table 2.

Landsat imagery was sourced from the USGS Earth Explorer platform, covering 2005 to 2024. All preprocessing and analysis were conducted using ERDAS Imagine 2020 and ArcGIS Desktop 10.7. This workflow ensures consistent data quality across years and supports robust spatiotemporal vegetation analysis [20].

Table. 2 NDVI Classification and Vegetation Density Interpretation

NDVI Range	Vegetation Density Class	Ecological Description
-0.19 to 0.08	Very Low Density	Water bodies, bare soil, urban surfaces, clouds, or snow
0.08 to 0.18	Low Density	Sparse vegetation, degraded land, grasslands, or fallow areas
0.18 to 0.24	Medium Density	Croplands, dry forests, or regenerating vegetation
0.24 to 0.31	High Density	Mixed deciduous forests or healthy agroforestry systems
0.31 to 0.51	Very High Density	Dense evergreen forest, mature forest canopy, high-biomass zones

Note: The NDVI classification thresholds presented in this table are informed by foundational principles in remote sensing science and have been further refined through empirical assessment of vegetation reflectance dynamics, calibrated against localized observations within the Phung River Basin. This approach ensures both alignment with globally recognized NDVI standards and sensitivity to the ecological heterogeneity inherent to the study area.

2.5 Ecological Classification of Vegetation Based on NDVI and Field Data

This study used an integrated method for vegetation classification that combined thematic vegetation maps from Thailand's Royal Forest Department and field survey data from the Phung River Basin vegetation was categorized into five ecologically distinct classes based on NDVI thresholds and field-verified land cover types:

1. **No Vegetation:** Barren land, urban surfaces, rocky zones, and water bodies (NDVI < 0.08).
2. **Sparse Vegetation:** Grasslands, shrublands, and degraded landscapes (NDVI 0.08 – 0.18).
3. **Moderate Vegetation:** Semi-natural rangelands and drought-tolerant croplands (NDVI 0.18 – 0.24).
4. **High Forest:** Mixed deciduous forests with partial canopy closure (NDVI 0.24 – 0.31).
5. **Dense Forest:** Evergreen forests with dense canopy cover (NDVI > 0.31).

This classification scheme was validated through high-resolution satellite imagery and spectral analysis, further supported by geospatial references from Google Earth. The methodological framework is conceptually aligned with advanced spatiotemporal data fusion approaches that integrate NDVI signals derived from multi-sensor platforms, including Landsat and Sentinel systems [23], [26].

2.6 Temporal NDVI Trend Analysis for Vegetation Dynamics (2005–2024)

This section provides a detailed classification of NDVI values to reveal spatial and temporal vegetation trends in the Phung River Basin from 2005 to 2024. The study utilized multi-temporal satellite imagery from Landsat 5 TM and Landsat 8 OLI-TIRS, which were geometrically and radiometrically corrected to ensure spectral comparability across years.

The standardized formula NDVI = (NIR - Red) / (NIR + Red) was used to work out the NDVI values, where NIR indicates the near-infrared and Red the red spectral bands [23].

Five bands, very low, low, medium, high, and very high, were used to categorize vegetation density based on ecologically validated NDVI thresholds- The classification employed the Maximum Likelihood Supervised Classification technique with a 70:30 training-to-testing ratio using ground-truth data, Google Earth imagery, and thematic land cover maps [23]. Classification accuracy was validated using confusion matrices, Overall Accuracy (OA), and the Kappa Coefficient.

The results highlight an increasing trend in high and very high NDVI classes, indicating ongoing vegetation recovery and successful land use regulation. Between 2005 and 2024, dense forest cover increased from 11.39% to 20.58%, while areas with very low-density vegetation slightly increased, reflecting residual land degradation in urbanized zones [25].

Table 3 and Fig. 3 collectively illustrate the annualized, NDVI-based vegetation data, which were systematically disaggregated to improve the clarity and interpretability of long-term vegetation dynamics. This disaggregation enables a more precise visualization of interannual variability and ecological transitions spanning from 2005 to 2024, thereby supporting a comprehensive temporal analysis. To further emphasize overarching trends in vegetation cover change, a linear trend line was

incorporated into Fig. 3. This improvement in graphics underscores the constant upward trend in dense vegetation classes, especially due to policy interventions after 2020, and improves the temporal readability of the dataset. Disaggregated temporal data and trend line visualization follow remote sensing analysis best practices and help researchers and land-use policymakers comprehend vegetation dynamics more intuitively. This analysis of NDVI trends provides essential insights for environmental monitoring, sustainable forest policy planning, and assessing ecosystem resilience in tropical transitional landscapes [19]. By examining NDVI trends, stakeholders can make informed decisions that foster environmental sustainability and improve the management of natural resources. This information is crucial for adapting strategies to mitigate the effects of climate change on these ecosystems.

Table. 3 NDVI Ranges and Vegetation Cover Percentages in the Phung River Basin (2005–2024)

Year	Very Low Density (-0.19 - 0.08)	Low Density (0.08 – 0.18)	Medium Density (0.18 – 0.24)	High Density (0.24 – 0.31)	Very High Density (0.31 – 0.51)
2005	5.84	28.06	32.86	21.86	11.39
2010	5.48	20.97	29.31	28.40	15.84
2015	5.43	21.46	28.49	22.57	22.04
2020	6.34	22.05	27.70	23.28	20.63
2024	6.20	21.81	28.68	22.72	20.58

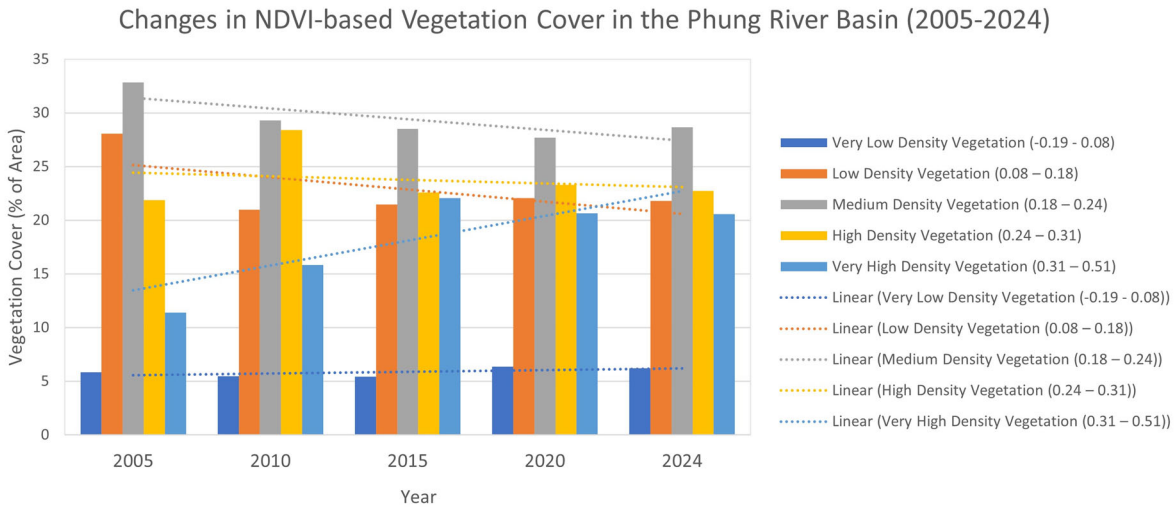

Fig. 3 Enduring trends for NDVI-derivative vegetation density in the Phung River Basin (2005–2024). Bars indicate percentages for annual vegetation class, while dotted lines reveal linear trend patterns, underscoring the dynamic range in high and very high-density flora over time.

2.7 Model Validation and NDVI Classification Thresholds

The Maximum Likelihood Supervised Classification method was used in this study to classify NDVI values across five defined vegetation density classes. To ensure statistical robustness and model generalizability, the dataset was partitioned into 70% training and 30% testing samples. Training data were derived from field survey observations, thematic vegetation maps from Thailand's Royal Forest Department, and high-resolution satellite imagery (e.g., Google Earth) were used to classify vegetation density.

To evaluate classification performance, confusion matrices were employed to compute the overall Accuracy (OA) and Kappa Coefficient (KC), two standard metrics widely accepted in remote sensing studies [30]. In Fig. 4, 130 accuracy assessment points were generated using the ArcGIS Accuracy Assessment Tool, stratified across all five observation years (2005, 2010, 2015, 2020, and 2024).

Beyond partitioning, NDVI classification was guided by ecologically relevant thresholds broadly accepted in remote sensing, reflecting consistent links between vegetation density and spectral response. The criteria for the five NDVI groups are defined as follows:

NDVI -0.19 to 0.08: Very Low Density (Water bodies, bare soil, built-up areas, and snow cover)

NDVI 0.08 to 0.18: Low Density (Sparse vegetation, dry grasslands, and degraded areas)

NDVI 0.18 to 0.24: Medium Density (Seasonal croplands, dry forests, or transitional vegetation)

NDVI 0.24 to 0.31: High Density (Healthy deciduous forests and agroforestry)

NDVI 0.31 to 0.51: Very High Density (Dense evergreen forest, mature canopy with high biomass)

This classification strategy aligns with spectral reflectance behavior and vegetation indices calibrated across tropical and semi-arid ecosystems, ensuring consistency with international remote sensing standards. The categorization also facilitates a longitudinal comparison of vegetation dynamics under anthropogenic and climatic pressures.

Substantial benefits in terms of monitoring vegetation over large spatial and temporal scales, particularly in areas difficult to access consistently, are possible by utilizing satellite-based remote sensing. A reliable, repeatable, and economical approach to evaluating vegetation dynamics is offered by the use of NDVI obtained from multispectral imagery. Satellite imagery enables landscape-scale surveillance at regular times, dissimilar to field-based methods that tend to be physically demanding, time-intensive, and spatially restricted. Although satellite data may be constrained by atmospheric disturbances and geographic resolution, it is easier to access, established, and less expensive than aerial surveys. Nevertheless, limitations exist with satellite-derived NDVI, such as atmospheric intrusion, sensor noise, and cloud defects that can impact precision. In this paper, meticulous preprocessing procedures, comprising Fmask for cloud masking and radiometric correction, were used to counter such limitations. Moreover, overall reliability was enhanced through the integration of field validation data that facilitated the calibration and verification of classification outputs. Remote sensing is an influential tool for long-standing environmental investigation when

combined with Geographic Information Systems (GIS). Even so, classification precision and ecological interpretation can be enhanced, particularly in heterogeneous or transitional environments, by combining satellite imagery with corresponding methods such as ground truthing and high-resolution aerial data.

2.8 Utilizing ΔNDVI for Change Detection

Change detection is critical in monitoring landscape transformation and ecological dynamics across time. This study applied NDVI-based change detection to evaluate temporal vegetation changes between years by calculating the difference in NDVI values (ΔNDVI) derived from multi-temporal satellite imagery. The methodology follows the post-classification comparison or map-to-map detection technique, where classified NDVI maps from different years are overlaid to identify specific change zones [27].

The formula used for detecting vegetation change through NDVI is as follows:

$$\Delta NDVI = NDVI_{t2} - NDVI_{t1} \quad (2)$$

Where:

$NDVI_{t2}$ = NDVI value at the more recent time point

$NDVI_{t1}$ = NDVI value at the earlier time point

An increase in vegetation cover was indicated by positive ΔNDVI values and loss or degradation by negative values [28]. This method ensures a straightforward and quantitative assessment of land cover dynamics using remote sensing data, which is particularly effective when using high temporal resolution sensors such as Landsat [18,25].

The integration of ΔNDVI analysis helps pinpoint areas of active reforestation, degradation, or transition, thus enabling policymakers to implement targeted conservation or restoration efforts. The results are visualized through change maps highlighting spatial transitions in vegetation density.

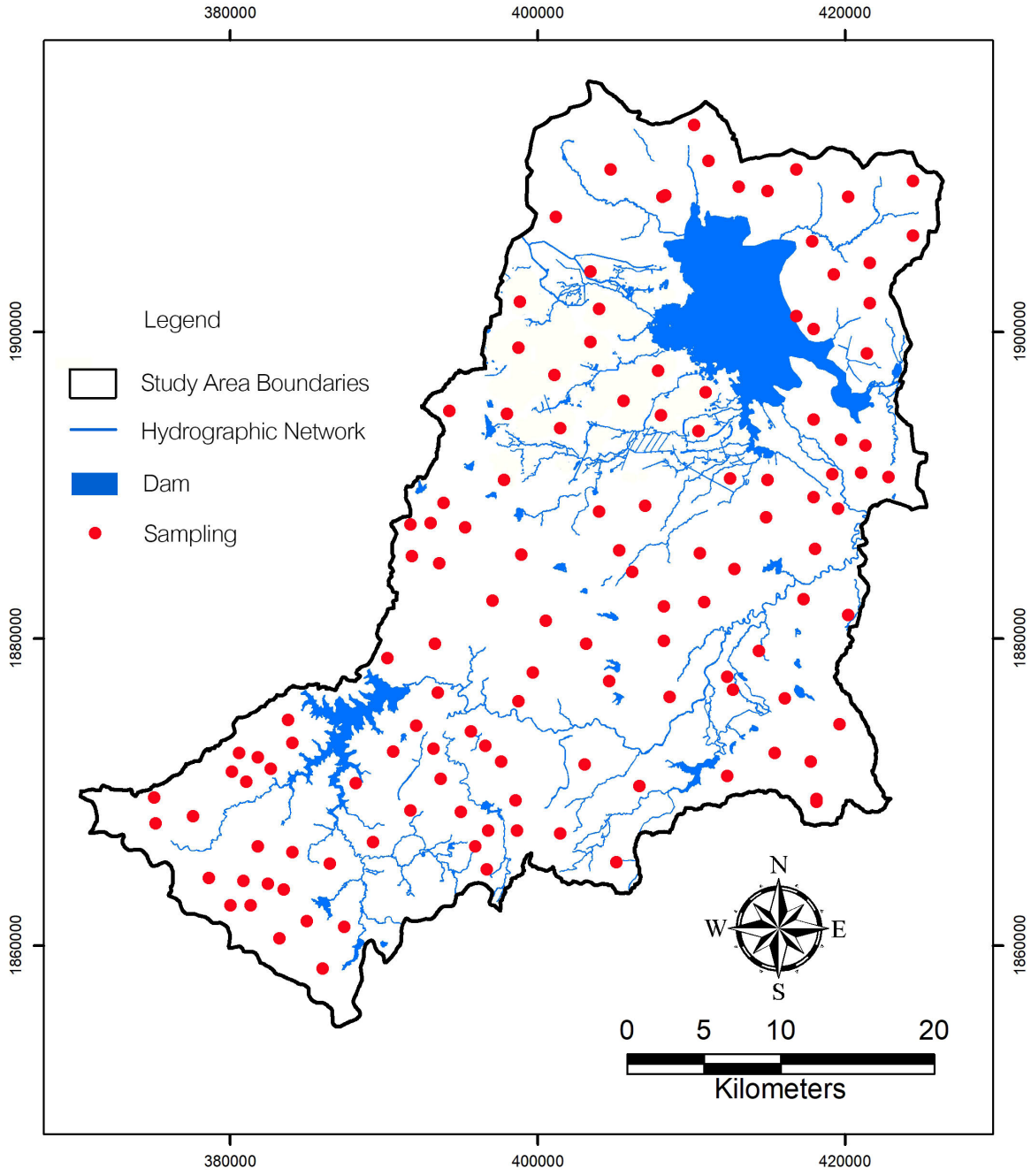

Fig. 4 illustrates the points of reference

3. Results and Discussion

The Phung River Basin, spanning an area of 1,639.60 square kilometers, has experienced significant changes in vegetation cover between 2005 and 2024. Five vegetation density classes, very low, low, medium, high, and very high, were detected based on the NDVI classification. Detailed trends over 19 years (total study period) are shown in Table 3 and Fig. 3.

In 2005, the majority of the basin was characterized by moderate-density vegetation (32.86%), followed by low-density (28.06%), high-density (21.86%), and very high-density (11.39%). By 2024, the proportion of very high-density vegetation increased notably to 20.58%, while moderate-density vegetation declined slightly to 28.68%. The share of low-density vegetation remained relatively stable, whereas very low-density vegetation increased marginally from 5.84% to 6.20%.

Although minor, this increase in very low-density vegetation indicates ongoing land degradation, likely due to urban expansion and persistent anthropogenic pressure in peripheral zones. On the other hand, the expansion of high and very high-density classes suggests partial ecological recovery, potentially driven by reforestation initiatives and stricter land-use regulations implemented post-2020. The relationship between demographic trends and vegetation change is particularly evident. From 2005 to 2020, rapid population growth in Sakon Nakhon Province contributed to deforestation and land conversion, reflected in fluctuating vegetation density. However, between 2020 and 2024, the population declined by 24%, coinciding with a stabilization in land-use practices and increased vegetation density in the upper NDVI classes. This suggests that demographic decline and environmental policies have positively influenced forest regeneration. Change detection through NDVI trends (Fig.4 and Fig.5) underscores the importance of temporal monitoring. The ΔNDVI analysis revealed zones of both degradation and regeneration, with more areas showing positive NDVI changes. Such results demonstrate the utility of NDVI as a tool for environmental management and policy planning, especially in transitional ecosystems.

Field authentication continues to be a vital component for guaranteeing the spatial accuracy of land cover classification, even though satellite remote sensing offers better spatial coverage and temporal resolution when evaluated against ground-based surveys and aerial imagery. Especially in heterogeneous settings where spectral uncertainty can occur frequently, the reliability of vegetation assessments can be enhanced by combining in-situ observations. The interplay between demographic shifts and vegetation dynamics is strikingly apparent. From 2005 to 2020, Sakon Nakhon Province experienced rapid population growth, which fueled deforestation, agricultural land conversion, and urban sprawl, thereby diminishing vegetation density in ecologically fragile zones. Conversely, between 2020 and 2024, the province witnessed a remarkable 24% population decline, coinciding with a shift in land-use practices and a notable increase in vegetation density, particularly in the higher NDVI classes. This finding strongly suggests that the combination of demographic contraction and robust environmental policies has had a positive influence on vegetation regeneration, most notably in the upper reaches of the watershed. Ultimately, this study confirms the critical role of NDVI-based monitoring in guiding sustainable resource management in vulnerable

watersheds like the Phung River Basin. Fig. 6 shows the 2024 NDVI values are appreciably greater than those in 2005, 2010, 2015, and 2020. The projected 2024 mean NDVI was 0.16, whilst the means for 2005, 2010, 2015, and 2020 were 0.14, 0.15, 0.11, and 0.15, respectively. The 2005 to 2024 Landsat image NDVI supervised classification facilitated observing and quantifying Phung River Basin forest cover growth, highlighting various changes over 19 years and producing high-quality maps (Fig. 5). This improvement is attributed to the timing of the satellite imagery captured during the dry period and the ensuing field corroboration. The 2005 classified NDVI accuracy was 93.07%, with a Kappa coefficient of 91.10%. For 2010, the accuracy was 90.77%, and the Kappa coefficient was 88.20%. In 2015, the accuracy reached 95.38%, with a Kappa coefficient of 94%. The 2020 accuracy was 93.08%, and the Kappa coefficient was 91%. The accuracy for the classified NDVI in 2022 is 96.15%, with a Kappa coefficient of 95% (Tables 4 to 8). These statistics indicate a trend of improving accuracy and reliability in the classification of NDVI over the years, with 2022 showing the highest accuracy and Kappa coefficient. This suggests that the methods used for classification have become more effective, leading to more precise assessments of vegetation health and coverage.

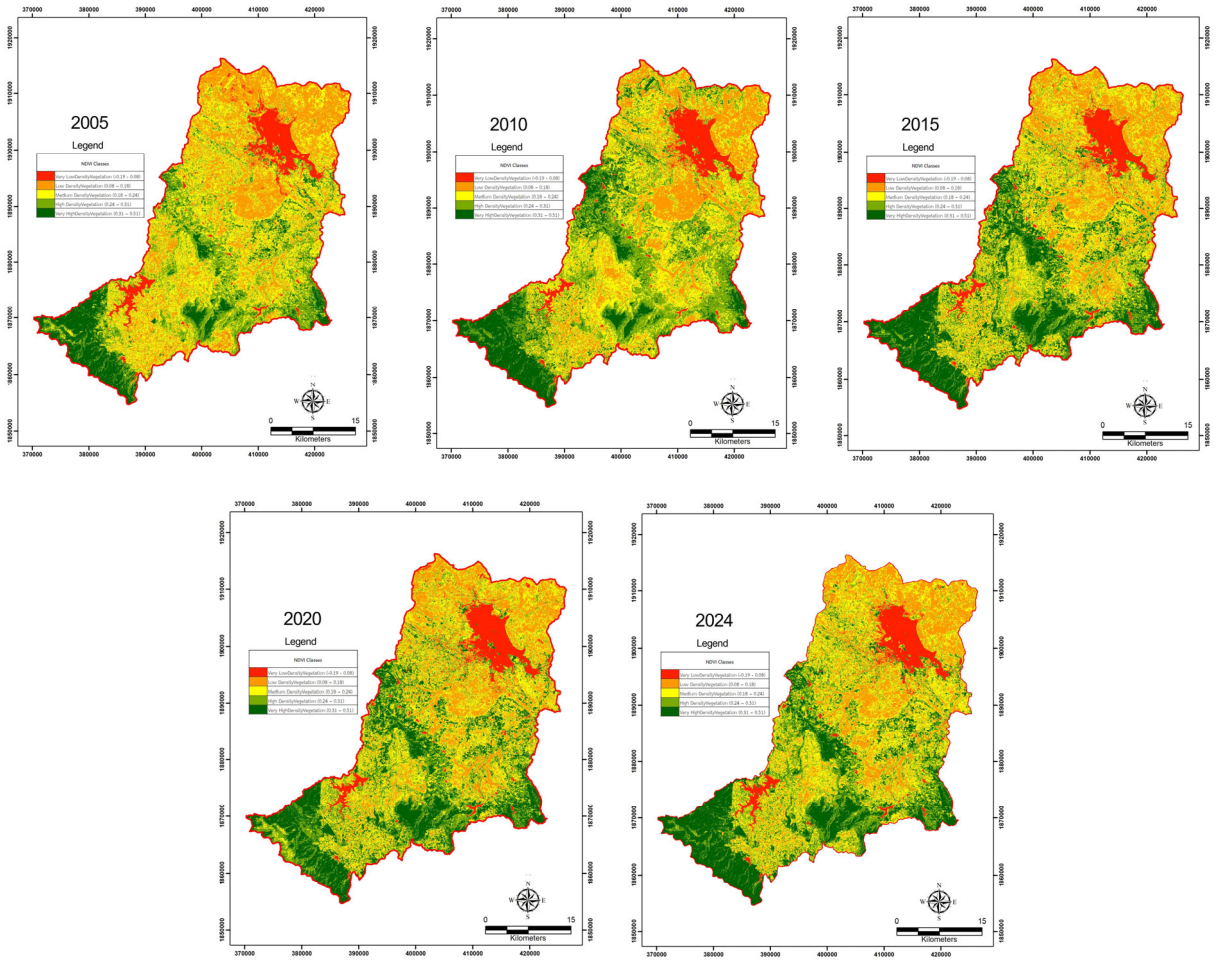

Fig. 5 Normalized Difference Vegetation Index (NDVI) maps for the Phung River Basin from 2005 to 2024, demonstrating spatial dispersal and the dynamics of vegetation density across five years of examination.

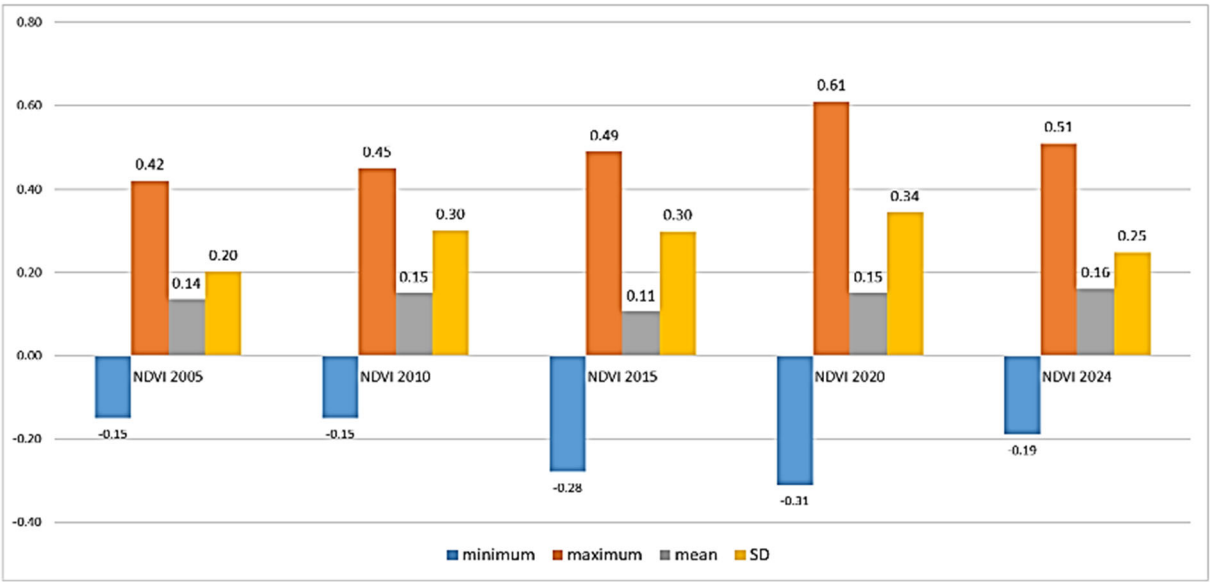

Fig. 6 NDVI values spanning the years 2005 to 2024

Table. 4 Assessment accuracy statistics for the NDVI (2005)

Classification	No vegetation	Sparse vegetation	Moderate vegetation	High vegetation	Dense vegetation	Total user	Use accuracy	Producer accuracy
No vegetation	34	2	0	0	0	36	94.44	97.14
Sparse vegetation	1	12	1	0	0	14	85.71	85.71
Moderate vegetation	0	0	34	2	0	36	94.44	97.14
High vegetation	0	0	0	21	3	24	87.50	91.30
Dense vegetation	0	0	0	0	20	20	100.00	86.95
Total	35	14	35	23	23	130	462.09	458.24
Overall accuracy (%)	93.07							
Kappa coefficient	91.10							

Table. 5 Assessment accuracy statistics for the NDVI (2010)

Classification	No vegetation	Sparse vegetation	Moderate vegetation	High vegetation	Dense vegetation	Total user	Use accuracy	Producer accuracy
No vegetation	34	1	1	0	0	36	94.44	97.14
Sparse vegetation	1	13	0	0	0	14	92.85	76.47
Moderate vegetation	0	3	31	2	0	36	86.11	91.17
High vegetation	0	0	2	21	1	24	87.50	87.50
Dense vegetation	0	0	0	1	19	20	95.00	95.00
Total	35	17	34	24	20	130	455.90	447.28
Overall accuracy (%)	90.77							
Kappa coefficient	88.20							

Table. 6 Assessment accuracy statistics for the NDVI (2015)

Classification	No vegetation	Sparse vegetation	Moderate vegetation	High vegetation	Dense vegetation	Total user	Use accuracy	Producer accuracy
No vegetation	35	0	1	0	0	36	97.22	100.00
Sparse vegetation	0	13	1	0	0	14	92.85	86.66
Moderate vegetation	0	2	34	0	0	36	94.44	91.89
High vegetation	0	0	0	24	0	24	100.00	96.00
Dense vegetation	0	0	1	1	18	20	90.00	100.00
Total	35	15	37	25	18	130	474.51	474.55
Overall accuracy (%)	95.38							
Kappa coefficient	94.00							

Table. 7 Assessment accuracy statistics for the NDVI (2020)

Classification	No vegetation	Sparse vegetation	Moderate vegetation	High vegetation	Dense vegetation	Total user	Use accuracy	Producer accuracy
No vegetation	32	3	1	0	0	36	88.88	96.96
Sparse vegetation	1	11	2	0	0	14	78.50	78.50
Moderate vegetation	0	0	36	0	0	36	100.00	90.00
High vegetation	0	0	0	23	1	24	95.83	100.00
Dense vegetation	0	0	1	0	19	20	95.00	95.00
Total	33	14	40	23	20	130	458.21	460.46
Overall accuracy (%)	93.08							
Kappa coefficient	91.00							

Table. 8 Assessment accuracy statistics for the NDVI (2024)

Classification	No vegetation	Sparse vegetation	Moderate vegetation	High vegetation	Dense vegetation	Total user	Use accuracy	Producer accuracy
No vegetation	36	0	0	0	0	36	100.00	97.29
Sparse vegetation	0	11	3	0	0	14	78.50	100.00
Moderate vegetation	1	0	35	0	0	36	97.22	89.74
High vegetation	0	0	1	23	0	24	95.83	100.00
Dense vegetation	0	0	0	0	20	20	100.00	100.00
Total	37	11	39	23	20	130	471.55	487.03
Overall accuracy (%)	96.15							
Kappa coefficient	95.00							

3.1 Spatiotemporal Dynamics of Vegetation Cover Based on NDVI Classification from 2005 to 2024

Table. 9 presents the NDVI classification statistics for 2005, 2010, 2015, 2020, and 2024.

Classification	NDVI 2005		NDVI 2010		NDVI 2015		NDVI 2020		NDVI 2024	
	area (km^2)	area (%)	area (km^2)	area (%)	area (km^2)	area (%)	area (km^2)	area (%)	area (km^2)	area (%)
No vegetation	95.70	5.84	89.81	5.48	89.09	5.43	104.03	6.34	101.63	6.20
Sparse vegetation	460.11	28.06	343.77	20.97	351.89	21.46	361.48	22.05	357.66	21.81
Moderate vegetation	538.73	32.86	480.57	29.31	467.20	28.49	454.21	27.70	470.23	28.68
High vegetation	358.35	21.86	465.72	28.40	369.99	22.57	381.67	23.28	372.60	22.72
Dense vegetation	186.71	11.39	259.74	15.84	361.44	22.04	338.21	20.63	337.48	20.58
Total	1639.60	100.00	1639.60	100.00	1639.60	100.00	1639.60	100.00	1639.60	100.00

Table 9 analyzes NDVI-based vegetation classification from 2005 to 2024, showing significant vegetation density changes in the study area; the “Dense vegetation” and “No vegetation” categories exhibited the most pronounced changes.

The area of dense vegetation increased markedly from 186.71 km² (11.39%) in 2005 to a peak of 361.44 km² (22.04%) in 2015 before showing a slight decline to 337.48 km² (20.58%) in 2024. This trend may reflect afforestation efforts, natural vegetation recovery, or land management policies implemented during the early 2010s. Conversely, the area with no vegetation showed minor fluctuations, peaking at 6.34% in 2020 before slightly decreasing to 6.20% in 2024. These changes might be linked to urban expansion or land degradation due to unsustainable agricultural practices. The “Sparse vegetation” and “Moderate vegetation” classes demonstrated relatively stable patterns, with slight declines in earlier years followed by stabilization. Sparse vegetation decreased from 28.06% in 2005 to around 21.81% in 2024, while moderate vegetation slightly declined but rebounded marginally by 2024.

3.2 Spatiotemporal Analysis of Vegetation Change Based on NDVI-Derived ΔNDVI Metrics (2005–2024)

Table. 10 Alterations in the area of vegetation category between 2005 and 2024

Classification	Change detection between 2005 and 2024	
	area (km^2)	area (%)
No vegetation	5.93	0.36
Sparse vegetation	-102.46	-6.25
Moderate vegetation	-68.50	-4.18
High vegetation	14.25	0.87
Dense vegetation	150.77	9.20
Total	0.00	0.00

The Phung River Basin spatiotemporal analysis of Vegetation dynamics from 2005 to 2024, as assessed via NDVI-based remote sensing, reveals distinct patterns of ecological transformation across the landscape. According to Table 10, the most notable change occurred in the "Dense vegetation" class, which expanded by 150.77 km² or 9.20% of the total basin area. This increase is likely to reflect effective reforestation campaigns, natural vegetative succession, and the implementation of more rigorous land-use policies in the post-2020 period. Conversely, both "Sparse vegetation" and "Moderate vegetation" classes exhibited significant reductions—by 102.46 km² (−6.25%) and 68.50 km² (−4.18%), respectively—suggesting a transition of semi-natural and agricultural lands into degraded or urbanized states.

Interestingly, the "No vegetation" category experienced a modest increase of 5.93 km² (0.36%) despite a 24% population decline between 2020 and 2024. This paradox suggests that land degradation and anthropogenic pressure may persist independently of demographic trends, possibly due to legacy land use, infrastructure expansion, or lack of ecological recovery mechanisms.

The NDVI change detection (ΔNDVI) results, as summarized in Table 11, highlight a nearly symmetrical pattern of ecological shifts: 170.96 km² (10.43%) of the area showed a positive NDVI change—indicating recovery—while 170.95 km² (10.42%) showed a negative change—indicating degradation. The remaining 1,297.69 km² (79.15%) exhibited no significant change. This duality suggests a transitional ecological state with simultaneous processes of forest regeneration and degradation occurring in different zones.

These findings affirm the utility of NDVI-based analysis in identifying subtle but ecologically significant vegetation shifts. They also underscore the value of continuous satellite-based monitoring in guiding sustainable landscape management, particularly in environmentally sensitive and demographically dynamic regions like the Phung River Basin. Taken as a whole, the findings demonstrate how vegetation cover changed dynamically during the course of the study, influenced by changes in land use, variations in the climate, and decisive efforts toward preservation. NDVI data were coordinated into five-year periods for enhanced interpretability (2005, 2010, 2015, 2020, and 2024), supporting the comprehensible conception of trends. To highlight key ecological changes,

especially an abrupt increase in dense vegetation between 2005 and 2015 and the ensuing stabilization seen after 2020, data were also categorized by classes of vegetation density.

The results by Lopes et al. (2024), who described forest recovery determined by policy mediation are in line with the rise in dense vegetation perceived in the Phung River Basin from 2005 to 2024. However, other studies detected decreasing forest NDVI trends in Eastern Europe, mainly because of sustained drought and the expansion of land use, such as the study by Prăvălie et al. (2022). The significance of local context in regulating vegetation consequences is highlighted by this distinction and emphasizes the achievement of recent preservation efforts in the Phung River Basin.

Table. 11 NDVI-based vegetation change detection from 2005 to 2024

Type of change	area (km^2)	area (%)
Positive	170.96	10.43
Negative	-170.95	10.42
No change	1297.69	79.15
Total	1639.60	100.00

4. Conclusion

This study provides evidence of significant vegetation changes in the Phung River Basin between 2005 and 2024, based on NDVI-derived satellite analysis. Notably, dense vegetation areas increased from 11.39% to 20.58%, while sparse and moderate vegetation areas declined. These findings align with earlier studies, such as Lopes et al. (2024), which reported that NDVI effectively captures post-disturbance forest recovery, and Prăvălie et al. (2022), who demonstrated that land-use and climatic changes were involved in forest NDVI trends.

The relationship between vegetation dynamics and population growth is particularly evident. Between 2005 and 2020, a growing population drove forest encroachment, agricultural expansion, and urbanization, reducing vegetation density in ecologically sensitive areas. In contrast, from 2020 to 2024, the population declined by 24%, coinciding with the implementation of more stringent zoning and environmental regulations. This demographic shift, combined with policy interventions, is likely to have facilitated vegetation regeneration—especially in the upper watershed.

Overall, this study underscores the practical relevance of NDVI-based change detection as a reliable method for long-term ecological monitoring. The findings offer valuable insights for policymakers, particularly in designing sustainable land use strategies and reforestation efforts. Moreover, the methodology employed in this research is transferable to other tropical basins in Southeast Asia, enabling broader application in climate-resilient landscape management and biodiversity conservation planning.

The outcomes of this study provide valuable insights for shaping policy frameworks aimed at forest conservation and ecological restoration on a regional scale, especially within ecologically

vulnerable areas. Incorporating NDVI-derived data into land-use planning processes will significantly strengthen the efficacy of systematic approaches to natural resource management.

5. Acknowledgement

The authors gratefully acknowledge the Groundwater Resources Institute, Faculty of Engineering, Khon Kaen University, for providing essential geospatial data and technical support. Appreciation is also extended to the Royal Irrigation Department for supplying critical datasets and instrumentation that supported the successful completion of this study.

6. References

[1] K. Mehmood et al., "Analyzing vegetation health dynamics across seasons and regions through NDVI and climatic variables," *Scientific Reports*, vol. 14, no. 11775, May 2024.

[2] Visual Capitalist, *"Which Countries Have the Largest Forests?"* [Online]. Available: https://www.visualcapitalist.com/which-countries-have-the-largest-forests/. (Accessed: December 20, 2024).

[3] Seub Nakhasathien Foundation, *"Forest and environmental situation 2023"* [Online]. Available: https://www.seub.or.th/forest-environmental-2023/. (Accessed: December 20, 2024).

[4] G. Aziz, N. Minallah, A. Saeed, J. Frnda, and W. Khan, "Remote sensing based forest cover classification using machine learning," *Scientific Reports*, vol. 14, no. 69, January 2024.

[5] M. Konatowska, A. Młynarczyk, W. Kowalewski, and P. Rutkowski, "NDVI as a potential tool for forecasting changes in geographical range of sycamore (Acer pseudoplatanus L.)," *Scientific Reports*, vol. 13, no. 19818, November 2023.

[6] C. Suwanprasit and N. Shahnawaz, "Mapping burned areas in Thailand using Sentinel-2 imagery and OBIA techniques," *Scientific Reports*, vol. 14, no. 9609, April 2024.

[7] W. Han et al., "Assessment of vegetation drought loss and recovery in Central Asia considering a Comprehensive Vegetation Index," *Remote Sensing of Environment*, vol. 16, no. 22, p. 4189, November 2024.

[8] K. Kulesza and A. Ho**Ś**ciło, "Influence of climatic conditions on Normalized Difference Vegetation Index variability in forest in Poland (2002–2021)," *Meteorological Applications*, vol. 30, no. 5, September 2023.

[9] J. Mašek, J. Tumajer, J. Lange, R. Kaczka, P. Fišer, and V. Treml, "Variability in tree-ring width and NDVI responses to climate at a landscape level," *Ecosystems*, vol. 26, no. 5, pp. 1144–1157, January 2023.

[10] P. Hajek et al., "Quantifying the influence of tree species richness on community drought resistance using drone-derived NDVI and ground-based measures of Plant Area Index and leaf chlorophyll in a young tree diversity experiment," *European Journal of Forest Research*, vol. 143, no. 1, pp. 141–155, October 2023.

[11] Thai Meteorological Department, *"Thai Meteorological Department: Sakon Nakhon Province Weather"* [Online]. Available: https://www.tmd.go.th/weather/province/sakon-nakhon. (Accessed: December 20, 2024).

[12] D. Udoma-Michaels and O. Akinola, "Analysis of Vegetation Index of Protected Forests in Akwa Ibom State, Nigeria between 2000 and 2021," *OALib*, vol. 09, no. 06, pp. 1–17, January 2022.

[13] E. Rahimi, P. Dong, and C. Jung, "Global NDVI-LST Correlation: Temporal and Spatial Patterns from 2000 to 2024," *Environments*, vol. 12, no. 2, pp. 67, February 2025.

[14] J. D. Stamford, S. Vialet-Chabrand, I. Cameron, and T. Lawson, "Development of an accurate low cost NDVI imaging system for assessing plant health," *Plant Methods*, vol. 19, no. 9, January 2023.

[15] S. Erasmi, M. Klinge, C. Dulamsuren, F. Schneider, and M. Hauck, "Modelling the productivity of Siberian larch forests from Landsat NDVI time series in fragmented forest stands of the Mongolian forest-steppe," *Environmental Monitoring and Assessment*, vol. 193, no. 4, March 2021.

[16] F. Maselli, M. A. Gilabert, and C. Conese, "Integration of high and low resolution NDVI data for monitoring vegetation in Mediterranean environments," *Remote Sensing of Environment*, vol. 63, no. 3, pp. 208–218, March 1998.

[17] T. T. Wahelo, D. A. Mengistu, and T. M. Merawi, "Spatiotemporal trends and drivers of forest cover change in Metekel Zone forest areas, Northwest Ethiopia," *Environmental Monitoring and Assessment*, vol. 196, no. 12, November 2024.

[18] E. Vera et al., "Change of vegetation cover and land use of the Pómac forest historical sanctuary in northern Peru," *International Journal of Environmental Science and Technology*, vol. 21, no. 14, pp. 8919–8930, April 2024.

[19] J. Doornbos, Ö. Babur, and J. Valente, "Evaluating Generalization of Methods for Artificially Generating NDVI from UAV RGB Imagery in Vineyards," *Remote Sensing*, vol. 17, no. 3, p. 512, February 2025.

[20] L. F. Lopes, F. S. Dias, P. M. Fernandes, and V. Acácio, "A remote sensing assessment of oak forest recovery after postfire restoration," *European Journal of Forest Research*, vol. 143, no. 3, pp. 1001–1014, March 2024.

[21] A. M. Khutuev, A. Kh. Zanilov, D. A. Tutukova, and I. Yu. Savin, "NDVI of crops as a remote indicator of arable soils quality," *Dokuchaev Soil Bulletin*, no. 121, pp. 70–85, December 2024.

[22] R. Prăvălie et al., "NDVI-based ecological dynamics of forest vegetation and its relationship to climate change in Romania during 1987–2018," *Ecological Indicators*, vol. 136, p. 108629, February 2022.

[23] M. T. Bhatti, H. Gilani, M. Ashraf, M. S. Iqbal, and S. Munir, "Field validation of NDVI to identify crop phenological signatures," *Precision Agriculture*, vol. 25, no. 5, pp. 2245–2270, July 2024.

[24] S. Xu, D. Wang, S. Liang, Y. Liu, and A. Jia, "Assessment of gridded datasets of various near surface temperature variables over Heihe River Basin: Uncertainties, spatial heterogeneity and clear-sky bias," *International Journal of Applied Earth Observation and Geoinformation*, vol. 120, p. 103347, May 2023.

[25] S. Ehsan and D. Kazem, "Analysis of land use-land covers changes using normalized difference vegetation index (NDVI) differencing and classification methods," *African Journal of Agricultural Research*, vol. 8, no. 37, pp. 4614–4622, September 2013.

[26] B. Mishra and T. B. Shahi, "Deep learning-based framework for spatiotemporal data fusion: an instance of Landsat 8 and Sentinel 2 NDVI," *Journal of Applied Remote Sensing*, vol. 15, no. 03, September 2021.

[27] S. Desai, M. Mattoo, A. M. Deshpande, A. Dey, and S. Akiwate, "Vegetation change detection through NDVI analysis using Landsat-8 data," in *Proceedings of the IEEE International Conference on Computing, Communication, and Information Technology (C3IT)*, Adisaptagram, Kolkata, India, March 9–10, 2024, pp. 1–6.

[28] S. Eskandari and S. K. Bordbar, "Provision of land use and forest density maps in semi-arid areas of Iran using Sentinel-2 satellite images and vegetation indices," *Advances in Space Research*, vol. 75, no. 3, February 2025.

[29] F. Ghilardi, S. De Petris, V. Torti, C. Giacoma, and E. Borgogno-Mondino, "A possible role of NDVI time series from Landsat Mission to characterize lemurs habitats degradation in Madagascar," *The Science of the Total Environment*, vol. 974, p. 179243, March 2025.

[30] R. G. Congalton and K. Green, *Assessing the Accuracy of Remotely Sensed Data*, 3rd ed. Boca Raton, FL, USA: CRC Press, 2019.

[31] Z. Zhu and C. E. Woodcock, "Object-based cloud and cloud shadow detection in Landsat imagery," *Remote Sensing of Environment*, vol. 118, pp. 83–94, December 2011.

[32] S. Foga et al., "Cloud detection algorithm comparison and validation for operational Landsat data products," *Remote Sensing of Environment*, vol. 194, pp. 379–390, April 2017.

[33] Z. Zhu, S. Wang, and C. E. Woodcock, "Improvement and expansion of the Fmask algorithm: cloud, cloud shadow, and snow detection for Landsats 4–7, 8, and Sentinel 2 images," *Remote Sensing of Environment*, vol. 159, pp. 269–277, January 2015.

[34] U.S. Geological Survey, *"Landsat Surface Reflectance"* [Online]. Available: https://www.usgs.gov/landsat-missions/landsat-surface-reflectance. (Accessed: October 23, 2024).

[35] N. Gorelick, M. Hancher, M. Dixon, S. Ilyushchenko, D. Thau, and R. Moore, "Google Earth Engine: Planetary-scale geospatial analysis for everyone," *Remote Sensing of Environment*, vol. 202, pp. 18–27, July 2017.

[36] Forest Research and Development Office, *"Forestry in Thailand"* [Online]. Available: https://forprod.forest.go.th/forprod/ebook/การป่าไม้ในประเทศไทย/Forest%20in%20thailand%20eng.pdf. (Accessed: April 14, 2025).

[37] NASA, *"Landsat Satellites"* [Online]. Available: https://landsat.gsfc.nasa.gov/satellites/. (Accessed: May 14, 2025).